CHEMICAL PHYSICS

Salt creeping as a self-amplifying crystallization process

M. J. Qazi, H. Salim, C. A. W. Doorman, E. Jambon-Puillet*, N. Shahidzadeh†

Salt creeping is a ubiquitous phenomenon in which crystals precipitate far from an evaporating salt solution boundary, which constitutes a major problem in outdoor electronics, civil engineering, artworks, and agriculture. We report a novel experimental approach that allows to quantitatively describe the creeping mechanism and demonstrate its universality with respect to different salts. We show that there exists a critical contact angle below which salt creeping occurs, provided also the nucleation of multiple crystals is favored. The precipitation of new crystals happens ahead of the contact line by the meniscus that progressively advances over the crystals forming also nanometric precursor films. This enlarges the evaporative area, causing an exponential increase in the crystal mass in time. The self-amplifying process then results in a spectacular three-dimensional crystal network at macroscopic distances from the solution reservoir. These findings also allow us to control the creeping by using crystallization modifiers.

INTRODUCTION

Salt creeping happens when crystals precipitate from evaporating salt solutions, a quite common phenomenon in everyday life. The deposited salt crystals can climb onto solid surfaces and spread far away from the solution. It is both a fascinating phenomenon and a major nuisance in many practical situations, causing, for example, corrosion of outdoor electronics and the buildup of crusts in saltwater aquariums. Because of the spreading of salt solution due to creeping, even a well-protected surface can corrode in a very short time (*1*). This spreading is very rapid and has even been compared to the phenomenon of superfluid film flow of helium (*2*). In porous materials, the transport of saline solution by creeping can lead to the physiological aridness of the soil above ground water level and the weathering of cultural heritage (*3*–*5*). The white stains on top of monuments and artworks (e.g., frescoes) are invariably due to salt creeping, and the resulting salt crystallization not only affects the aesthetics but can also even cause damage to the material, such as cracks and delamination.

Since the first paper on the existence of this phenomenon by Washburn almost 100 years ago (*6*), very few studies have been dedicated to understand the driving forces for the initiation and rapid growth of salt creeping. It was initially suggested that liquid capillary bridges between the crystals and the solid surface were the primary driving force for the onset of creeping (*6*). Subsequently, another key factor was identified: The ability of the crystal to adhere to the substrate determines whether a particular salt creeps on a particular substrate (*7*). Recently, the flow of a solution film over the crystallites adhering to the surface was proposed to facilitate crystal growth beyond the solution boundary (*8*). However, a quantitative description of the creeping mechanism and its universality with respect to different salts is still missing. This quantitative description is needed for predicting and quantifying the speed of growth and, consequently, controlling the creeping process to avoid its negative impact in practice. Here, we pursue such an explanation for different salts and further demonstrate a way to control salt creeping using crystallization modifiers.

Institute of Physics, University of Amsterdam, Science Park 904, 1098 XH, Amsterdam, Netherlands.
*Present address: Department of Chemical and Biological Engineering, Princeton University, Princeton, NJ 08540, USA.
†Corresponding author. Email: n.shahidzadeh@uva.nl

RESULTS

We performed creeping experiments in which a vertical glass rod (hydrophilic substrate, diameter d = 6 mm) is brought into contact with one of the four homogeneous undersaturated salt solutions: NaCl, KCl, and two types of sodium sulfate, Na_2SO_4-A (precipitating in the form of hydrated crystals) and Na_2SO_4-B (precipitating in the form of anhydrous crystals) (*9*). The solutions were left to dry in a controlled climatic chamber. At a relative humidity (RH) of 40% and temperature of 21°C, no salt creeping on the cylindrical substrate was observed for any of the solutions studied: During evaporation, the salt concentration increases, and after reaching the saturation concentration, crystals nucleate either in the reservoir (for Na_2SO_4-B) or at the liquid/air interface (for NaCl, KCl, and Na_2SO_4-A). The latter crystals subsequently grow and fall into the reservoir where they continue to grow as time progresses. As the level of the solution in the reservoir decreases with evaporation time, the solution detaches from the glass rod without any creeping.

In contrast, at a low RH of ~6%, salt creeping is observed for all salt solutions (see Fig. 1 and movies S1 to S3). Before the start of creeping, the solution first reaches saturation, triggering crystal precipitation and growth in the reservoir, just as observed for a RH of 40%. However, as evaporation continues, creeping on the vertical glass substrate can be observed to start with the precipitation of new crystals at the liquid/air interface close to the contact line: A chain of crystals grows outside of the contact line and moves upward onto the glass substrate. For Na_2SO_4-B, creeping is observed as soon as first crystals precipitate at the contact line on the solid/liquid interface, where the evaporation rate is highest. Our results show that these salts creeping at low RH is a general phenomenon as it can also be seen on a thinner glass rod (diameter = 3 mm) as well as on glass slides (flat surfaces) (see the Supplementary Materials).

To investigate the mechanism of creeping, we first analyze the contact angle of each salt solution meniscus with the substrate. Figure 2 shows the evolution of contact angle with time during evaporation; because the contact line is pinned to the glass substrate (see the Supplementary Materials), evaporation leads to a decrease in the contact angle (Fig. 2C).

For NaCl, KCl, and Na_2SO_4-A solutions, for which crystal precipitation starts at the liquid/air interface (see Materials and Method), our results show that there is a critical contact angle that needs to be reached to initiate salt creeping on the substrate. Moreover, this

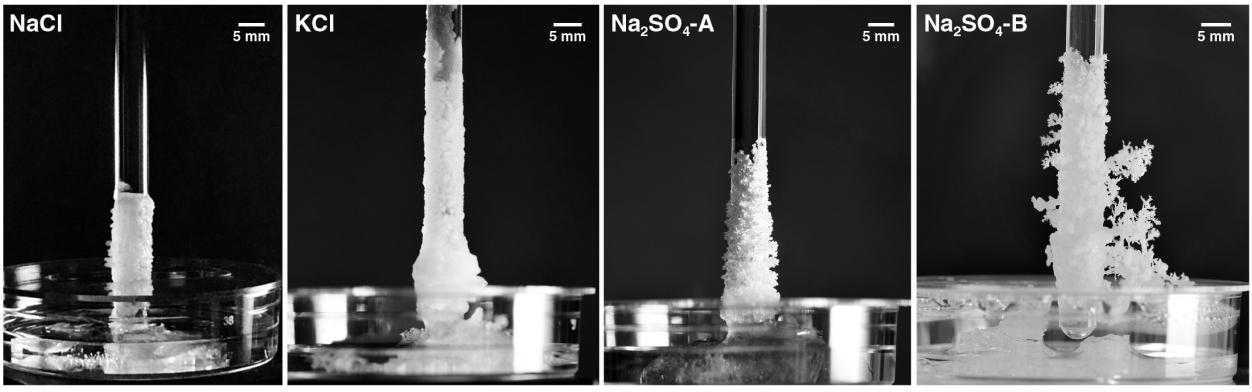

Fig. 1. Creep left by different salts. Photographs of the salt creep at the end of the creeping process, when all the solution has evaporated. Solutions (from left to right): NaCl, KCl, Na_2SO_4-A, and Na_2SO_4-B. For all experiments: RH = 6% and T = 21°C.

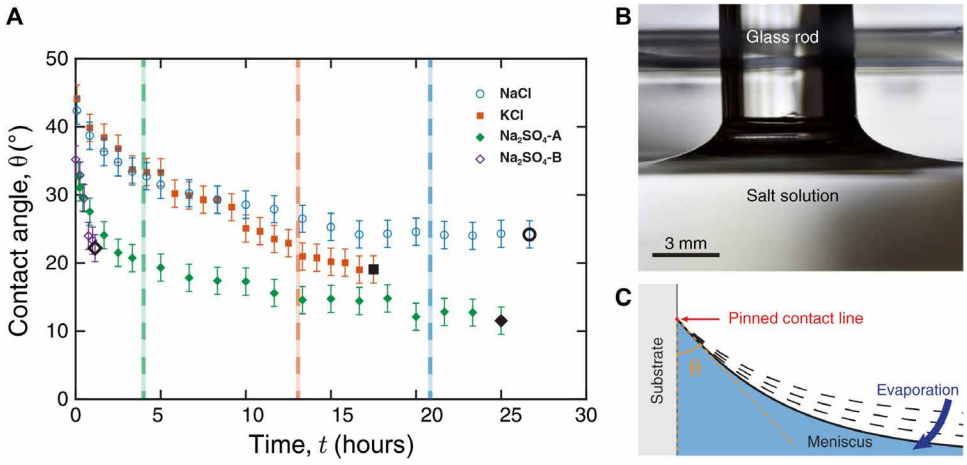

Fig. 2. Contact angle evolution of the salt solutions. (**A**) Time evolution of the contact angle θ of the liquid meniscus for the four salt solutions under study as they evaporate (RH = 6% and T = 21°C). The dashed lines indicate the time at which precipitation starts in the solution. The creeping on the rod starts right after the last data point (highlighted in black). (**B**) Typical photograph of the meniscus, as used to determine the contact angles. (**C**) Schematic of the meniscus evolution as the solution evaporates.

critical contact angle is found to be lower for salt solutions with a lower liquid/vapor surface tension, i.e., lower solubility. For Na_2SO_4-B, creeping starts immediately at the start of the experiments with the first crystals precipitating at the solid/liquid interface at a contact angle around 23°. It is important to note that the value of the critical angle for a given salt is found to be independent of the substrate curvature (radius of curvature r = 3 and 6 mm for the two different rods and $r = \infty$ for the slides); the same range of value is obtained in all cases (see also the Supplementary Materials).

The sequence of steps leading to creeping and the role of the contact angle can be explained as follows. First, for the NaCl, KCl, and Na_2SO_4-A solutions, it is energetically favorable to nucleate at the liquid/air interface (*10*–*12*). Second, since the evaporation rate is highest at the three-phase contact line (*13*), this leads to a higher concentration of ions at this location and, hence, a higher probability of nucleation close to the contact line (*14*). The low RH enhances this process and results in a more heterogeneous solution with even more salt ions at the contact line, which, in turn, promotes the precipitation of multiple crystals. In evaporating drops, this can lead to the well-known "coffee stain effect," in which a ring of salt crystals forms at the pinned circular contact line. As illustrated in Fig. 3, the same thing happens in our experiments: During evaporation, crystals nucleate and grow near the meniscus at the liquid/air interface but then fall in the reservoir because of their weight (Fig. 3A). The process continues until the contact angle is such that the suspended growing crystals fit exactly into the liquid meniscus (Fig. 3B), preventing them from falling down; the crystal is subsequently confined within the liquid/air and solid/liquid interfaces (*7*). As the confined crystal is still in contact with the solution, a film of the solution wraps around it. Because of the high evaporation rate, new crystals rapidly form on top of the film, reaching higher than the earlier crystal, and a new advancing contact line is, thus, created by the advancing liquid (Fig. 3C). In this way, a chain of crystals grows upward along the cylindrical glass substrate. The crystals are kept from falling into the solution by capillary forces, exactly like the strong adhesion of two glass slides separated by a thin film of solution (*6*). In addition, the precipitation and growth of new crystals adhering on the glass surface add a certain roughness to the substrate, which makes the surface more wettable by enabling capillary flow (*15*). At a RH of 40%, evaporation is much slower, so before the critical contact angle is reached, the crystals have time to grow, move away from the contact line along the meniscus, and fall into the solution due to their increasing weight. Therefore, creeping is not observed on the substrate.

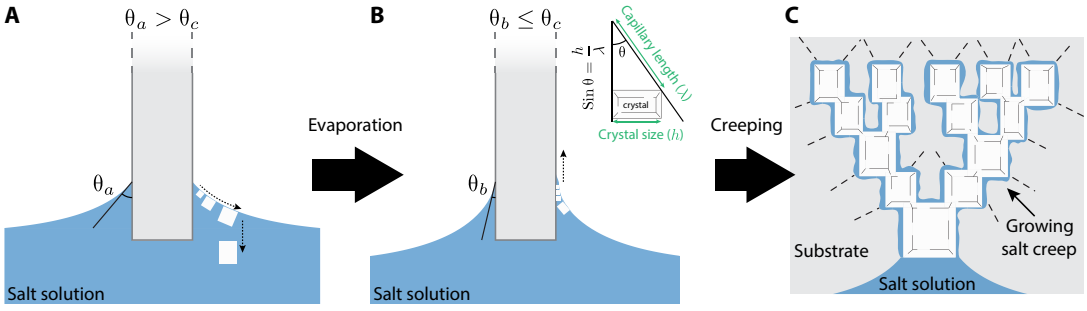

Fig. 3. Crystal precipitation during evaporation. (**A**) At high contact angles $\theta_a > \theta_c$, crystals forming on the meniscus fall into the bulk. (**B**) At lower contact angles $\theta_b \leq \theta_c$, the crystals are confined within the liquid/air and solid/liquid interfaces at the contact line. The inset shows the parameters used to calculate the typical crystal size at this onset of creeping. (**C**) Illustration of the creeping front and the self-amplified growth process: a single entrapped crystal in contact with the bulk solution (blue) gets covered by a thin film of solution from which new crystals grow ahead, and so forth.

For salts that nucleate and grow specifically at the solid/liquid interface, if conditions are such that multiple nucleation is promoted at the contact line, reaching a critical contact angle is not a necessary condition to promote the creeping, as the crystals are already confined at the contact line. This is exactly what we see at low RH for Na_2SO_4-B solutions: Creeping initiates very rapidly as soon as first crystals of anhydrous sodium sulfate crystals precipitate and grow at the solid/liquid interface close to the contact line.

As already mentioned, the creeping phenomenon is independent of the substrate curvature as the same critical contact angles are also observed for the flat glass slides and thinner glass rods (see the Supplementary Materials). Consequently, the initiation of creeping is determined primarily by the confinement of the nucleated crystal between the substrate and the liquid/air interface at the contact line (Fig. 3B). The effect of surface tension on the shape of this liquid/air interface is likely to dominate the effect of gravity when the interface's radius of curvature is much less than the capillary length. The latter, which controls the size of the meniscus, can be estimated for a given liquid by comparing the Laplace pressure to the hydrostatic pressure at a depth λ for a liquid of density ρ submitted to Earth's gravity $g = 9.8\ m/s^2$.

$$\lambda = \sqrt{\frac{\gamma}{\rho g}}$$

Here, γ is the liquid/vapor surface tension of the salt solution at saturation (see the Supplementary Materials). Thus, at scales smaller than the capillary length, gravity hardly affects the movement of the liquid. As a result, liquids can generally exhibit interesting behaviors such as moving up inclined planes or creeping up the sides of a small capillary tube.

Therefore, when the crystal is confined between the substrate and the liquid/air interface at these scales (Fig. 3B), the typical size (height) of the entrapped crystal can then be estimated, knowing the critical contact angle and the value of the capillary length for a given liquid according to the scheme of Fig. 3B

$$h = \lambda \sin\theta$$

where θ is the contact angle, h is the typical crystal size (height), and λ is the capillary length. The typical crystal size (height) is found to be between 0.5 mm for Na_2SO_4-A and 0.8 to 1 mm for KCl and NaCl, respectively.

To gain further insight into the creeping mechanism, we analyzed the rate of crystal growth on the substrate after the onset of creeping. The glass rod, acting as substrate to the crystal growth, is attached to a mass balance, allowing direct measurement the combined mass of salt crystals and thin film of solution on the substrate as a function of time. As shown in Fig. 4, this mass grows nonlinearly fast, suggesting that salt creep may be a self-amplified process, in which the crystal deposit grows, allowing the extension of the film of solution, which, in turn, triggers further crystal growth and so on (Fig. 3C). We model this growth by starting from the reasonable hypothesis that the rate of crystal precipitation is given by the evaporative surface area $A(t)$ of the film from which the crystals are growing: $\frac{dm}{dt} \sim A(t)$, with $m(t)$ as the mass of the creep crystals at time t. Precipitation is a multistep process; dissolved substances must be transported in the vicinity of the crystal surface, and then they must attach. When the limiting factor is the attachment step, the growth rate is proportional to the surface area of the crystal whatever the exact shape of the crystal.

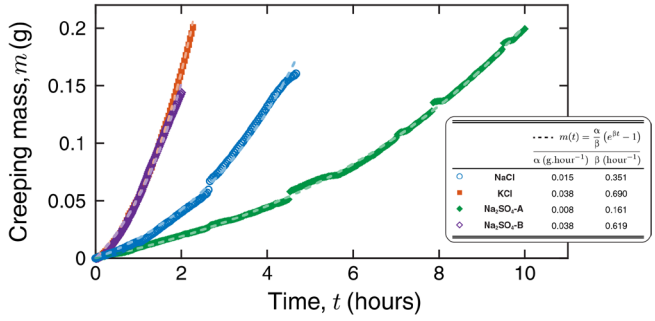

Fig. 4. Self-amplified growth. Mass of the salt creep on the glass rod as function of time for the four salts studied. Dashed curves are fits of the experimental data with Eq. 1. Fitting parameters are listed in the inset.

On the other hand, as the emergence of new crystals (i.e., secondary nucleation) ahead of the first precipitated crystal provides new surface area, A increases with the total mass of crystals that have already formed; this increases the evaporative area and, hence, the crystal precipitation. For a smooth surface growing in all directions, the mass should grow faster than the area. In our experiments, because the surface has many ramifications, the area will grow much faster than that of a smooth surface. For fractal objects, the area-to-mass ratio is roughly constant for a fractal dimension of two; such a fractal dimension is typical of diffusion-limited aggregation processes similar to the one here and then would lead to the

proportionality between the mass and surface area (*16*). By combining these equations, we get

$$\frac{dm(t)}{dt} = \alpha + \beta m(t)$$

which predicts an exponential growth of the form

$$m(t) = \frac{\alpha}{\beta}(e^{\beta t} - 1) \quad (1)$$

Here, α is a surface coefficient that depends on the initial conditions (through A_0) and varies with the geometry of the experiment, while β is a growth coefficient that only depends on the salt and describes how fast the creeping process proceeds. As shown in Fig. 4, our growth model fits our experimental data very well for the four different salts, thus confirming the validity of these hypotheses. Moreover, as expected, α varies between different experiments, but β is found to be an intrinsic property of each salt (see the Supplementary Materials).

It is hard to measure the rate of advancement of the creeping front, as the creeping grows in both vertical and lateral directions and varies randomly for a given salt and from one salt to another. However, an interesting observation is that we measure clear differences in growth rates for salts with similar physicochemical properties, namely, NaCl versus KCl and Na_2SO_4-A versus Na_2SO_4-B (see Fig. 4). Therefore, differences in creeping rates among salt materials could indicate differences in the shape and, hence, surface-to-volume ratio of the crystals. For example, the salt could form a more branched crystallization pattern with a higher number of smaller crystals.

To test this hypothesis, we took scanning electron microscopy (SEM) images of the salt creep at the end of the experiments to investigate its morphology. The results, shown in Fig. 5, reveal a clear difference in the number of crystals and the extent of branching between the different salts. The KCl solution leads to the precipitation of a large number of smaller crystals compared with the very similar NaCl solution, which explains its higher growth rate of creeping. The same applies to the Na_2SO_4-B solution, where the higher extent of branching of anhydrous sodium sulfate sodium (thenardite phase III) is consistent with the higher creeping rate of this salt solution compared with the hydrated form Na_2SO_4-A. Hydrated crystals of sodium sulfate are generally much larger in size than the anhydrous form and consequently lead to a less extensive surface area, explaining its smaller growth rate. The SEM images show the porous structure upon evaporation of the bound water, which leads to the loss of its fundamental hydrated structure (see Materials and Methods).

Our results suggest that the creeping of salts can be controlled by influencing the number of emerging crystals (i.e., the branching of the crystallization pattern) (*17*) and their size. To confirm our hypothesis and gain further insight into the creeping mechanism, we take two different types of additives (surfactants) known to affect salt crystallization and test their influence on the creeping of NaCl. We use CTAB (cetyltrimethylammonium bromide), which is cationic, and Tween 80, which is nonionic; these have been shown to act as either nucleation promoters or inhibitors for salt crystallization, rather than changing the wetting properties of these high-concentration salt solutions (*18*, *19*). Although the addition of surfactants to the salt solutions lowers their surface tension, it does not substantially affect the initial contact angle of the liquid with the substrate. However, CTAB has a promoting effect on the nucleation of NaCl at the liquid/air interface, while Tween 80 has an inhibitory effect (see fig. S2).

We repeated our creeping experiments for NaCl solutions with the two surfactants. As shown in Fig. 6A, CTAB promotes the creeping, while Tween 80 suppresses it. We plot in Fig. 6B the corresponding contact angle and creeping mass for these solutions. When Tween 80 is added to the solution, the contact angle continuously decreases

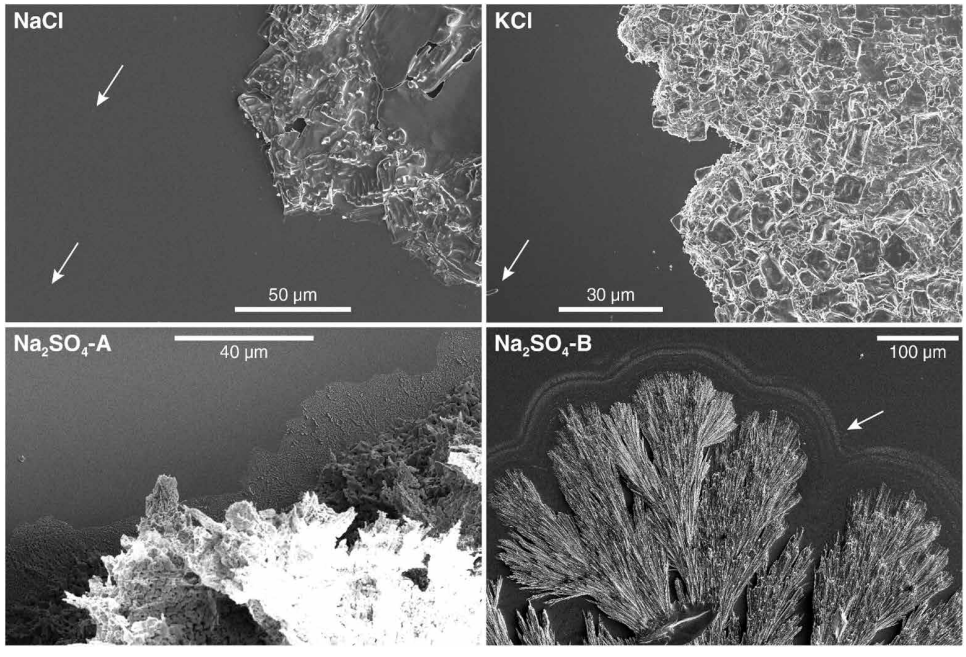

Fig. 5. Crystal shapes in salt creep. SEM images of creep formed from the four salt solutions. Note the different scales. The arrows indicate locations slightly ahead of the creep edge where high-resolution SEM revealed the presence of nanocrystals (see Fig. 6).

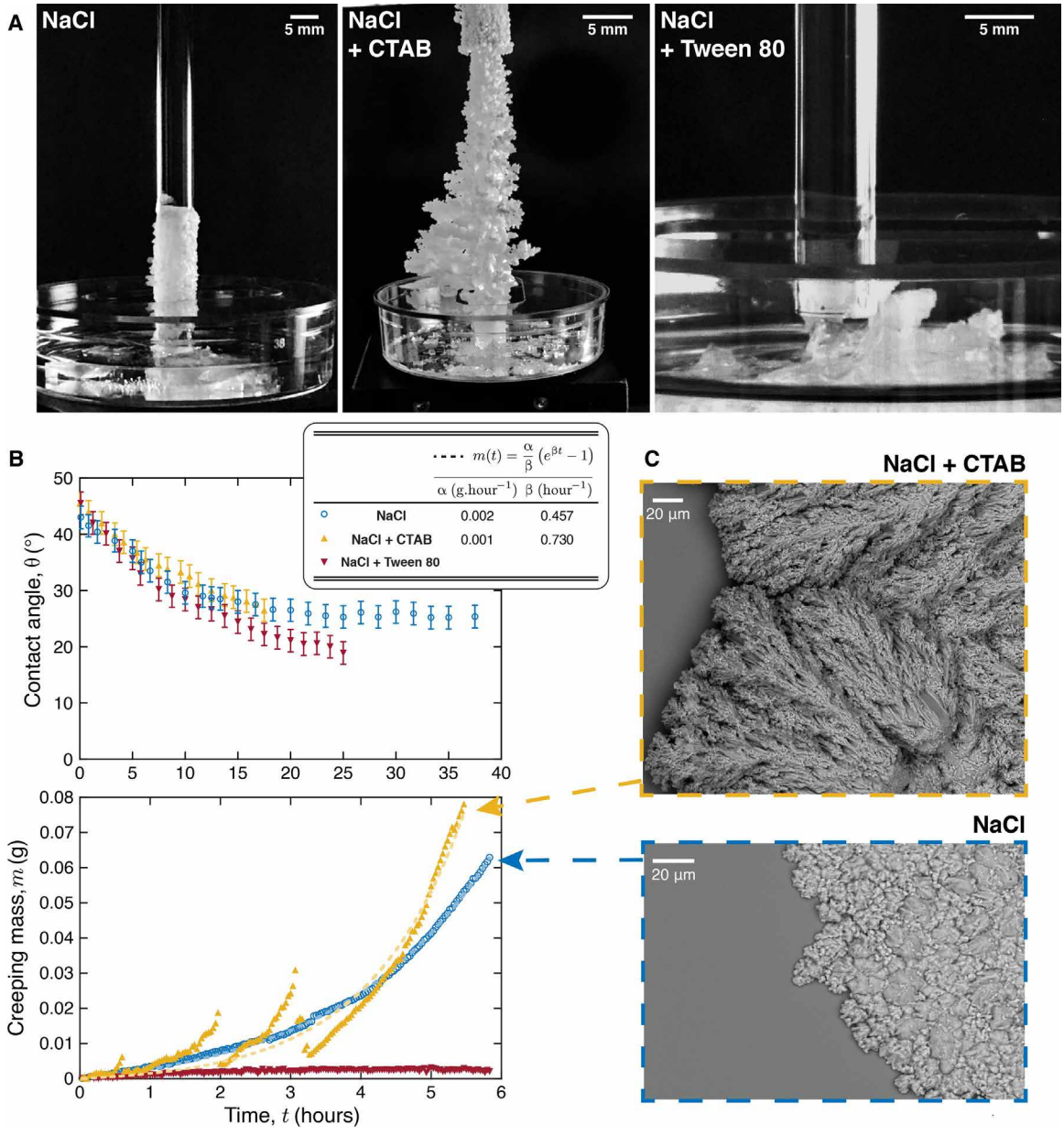

Fig. 6. Effect of surfactants on salt creeping. (**A**) Comparison of the final salt creep of NaCl solutions with and without the addition of CTAB or Tween 80 surfactants (RH = 6% and T = 21°C). (**B**) Time evolution of the contact angle (top) and creeping mass (bottom) for the same solutions as they evaporate. (**C**) SEM pictures of creep found for NaCl (bottom) and NaCl + CTAB (top).

until complete detachment of the liquid from the substrate without any creeping. On the other hand, when CTAB is used as additive, creeping is seen at a much earlier time, i.e., as soon as crystallization starts in the solution. As can be seen in Fig. 6B, the NaCl + CTAB creeping crystals grow and then slip and fall back into the solution, followed by a new creeping crystal that grows immediately without any delay after the slipping of the first crystal. The overall growth is much faster than without the CTAB. This stick-slip can lastly lead to the formation of a salt bridge between the bottom of the receptacle and the rod; the creep of the CTAB/salt then happens at a much higher rate than for the pure NaCl. The higher growth rate of creeping with CTAB is a signature of CTAB causing a faster increase in surface area, which is readily seen in photographs of the salt creep (Fig. 6A) and confirmed by high-resolution SEM (Fig. 6C). This increased surface area increases the evaporation and, hence, accelerates the creeping. It is also important to note that, in the presence of CTAB, creeping starts reproducibly at the same critical contact angle (25°) as the one observed for pure NaCl solution (Fig. 6B). This result confirms once again that for the onset of creeping, a critical contact angle needs to be reached to entrap the crystal and promote the multiple crystallization on the substrate.

Rationalizing our observations, because CTAB is a cationic surfactant, it can attract chloride as a counterion and consequently act as a nucleation site for the precipitation of NaCl. On the other hand,

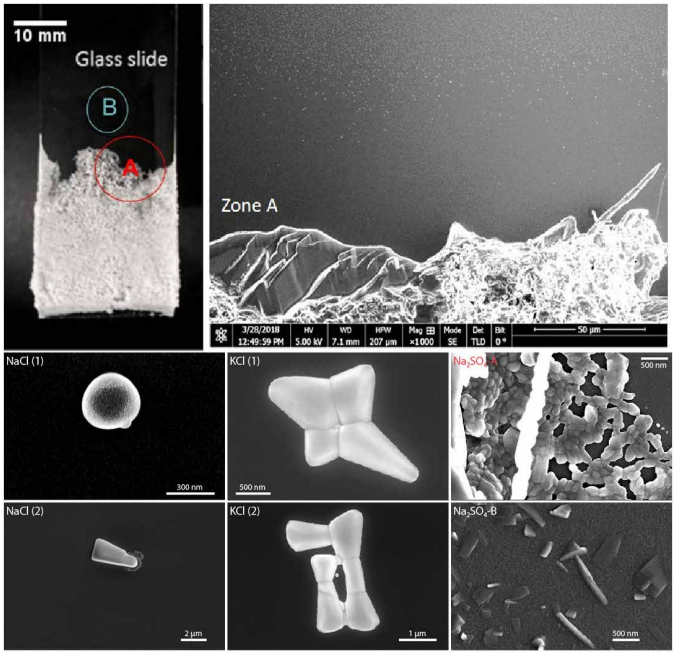

Fig. 7. Crystallization at the front of the creep zone. Top: Image of NaCl creep formed on a glass slide and zoom around the creep boundary with a high-resolution SEM (zone A). **Bottom**: High-resolution SEM images of nanocrystals spreading over the glass substrate from the precursor film (zone B) in regions beyond the creeping line (zone A) (also indicated by arrows in Fig. 5). Note the different scales. NaCl nanocrystal [panel NaCl (1)] initially without a well-defined structure, which could correspond to the amorphous state evolving toward whisker growth [panel NaCl (2)] from a thin film of solution, while KCl crystals are seen to grow by means of multiple nucleation even at an early stage of growth at the nanoscale [panels KCl (1) and (2)]. The precipitation of the whisker-shaped thenardite (anhydrous crystals) (some laying down and some pointing up) can also be seen for Na_2SO_4-B. Na_2SO_4-A forms a porous structure made of anhydrous nanocrystals upon removal of the bound water during the drying of the hydrated crystals (zone A).

Tween 80 is a nonionic surfactant, and consequently, it does not interact with the ions in the solution. One notable consequence of this is that adding NaCl in a Tween 80 solution does not change the CMC (critical micelle concentration) of this surfactant, whereas for CTAB, adding salt reduces the CMC, because the electrolytes screen the electrostatic interactions between the polar heads of this surfactant (*18*, *19*). The adsorption of CTAB at both interfaces (liquid/air and solid/liquid) then promotes the nucleation there, while the adsorption of Tween 80 inhibits it. Tween 80 induces the passivation of these locations for any crystal nucleation and consequently induces precipitation in the bulk rather than at the surfaces (see the Supplementary Materials); in this way, creeping can be avoided. On the contrary, for CTAB, the enhanced nucleation close to the contact line triggers the creeping earlier. The stick-slip motion during the growth of the NaCl + CTAB creep is likely due to the lower surface tension of the salt solution in the presence of CTAB, decreasing also the adhesive capillary force between the crystal and the glass substrate.

In principle, Marangoni flows due to concentration gradients could arise from the preferential evaporation at the meniscus and the presence of surfactants. However, in the context of creeping, we do not observe any influence of these flows, for several reasons:

(i) The salt concentration gradient between the solution film and the bulk is small because both are very close to saturation. The film being already in contact with the salt crystal would immediately form another crystal by secondary nucleation and, hence, cannot be highly supersaturated.

(ii) All the processes studied here are so slow (the typical experimental time scale is a day) that all concentration gradients have disappeared by diffusion. In addition, previous experiments and simulations (*14*) have already shown that in the case of salt solution, the ion concentration field near the contact line of a receding vertical meniscus in contact with a wall is not affected by convective motion. Subsequently, the large salt concentration near the contact line of a receding meniscus is not due to convection but rather due to the confinement effect and evaporation, as is the case here.

(iii) For salt solutions with surfactants, if these flows would have an impact on the creeping, this should then be observed for both surfactants. Our results show that with CTAB, creeping occurs, whereas when Tween 80 is added to the solution, no creeping occurs. Moreover, the contact angle at the initiation of creeping is the same in both the presence and absence of surfactants, showing again that the surfactants only intervene in the nucleation process.

Last, an important observation from the high-resolution SEM images at the edge of the creeping boundary (Fig. 7) is that multiple nanoscale salt crystallites form beyond the edge of the salt creep as evidenced by SEM images. This indicates that this region (zone B) was wet by a precursor film that extends far beyond the macroscopic contact line where the macroscopic crystals form (zone A). The existence of such a precursor film does not question the existence of a well-defined macroscopic contact angle of the liquid with the substrate at the contact line where the evaporation is highest and leads to crystal precipitation and creeping according to the proposed mechanism. It is well known that macroscopic droplets on surfaces (or any surface in contact with a liquid reservoir) are invariably accompanied by such a precursor film, the thickness of which is irrelevant for the dynamics of fluid motion (*20*, *21*). The creeping phenomena described in the paper happen on length scales of millimeters or larger, whereas the precursor film is nanometric.

The electron microscopy picture on Fig. 7 shows these nanocrystals ~100 μm far from the macroscopic contact line, and they can be seen up to a centimeter away from the contact line but are not observed close to the contact line. The empty region between the contact line and the nanocrystals is very much consistent with previous findings (*22*) that when a crystal nucleates somewhere and grows rapidly on a surface (in our case, at the creeping front), there is an empty region around it at the end of drying. This is because the initial rapidly growing crystal "eats up" the supersaturation around it.

It is also interesting to note that the whisker-shaped nanocrystals (*23*) are seen for most of the salts, although at an early stage of their formation, some peculiar shapes, resulting from crystal growth in a thin film of solution undergoing fast evaporation, can be observed. The precipitation of amorphous sodium chloride has been reported by supersonic spray drying at a much smaller scale (below 10 nm) (*24*). The observation of NaCl nanocrystals with similar shapes [Fig. 7 (1)], i.e., round without facets, but a much larger scale (here, 300 nm) could be an indication of the precipitation of amorphous phase in the thin film undergoing fast evaporation. The nanoprecursor films are usually very challenging to observe experimentally; salt creeping shows that the film can be probed thanks to nanocrystal precipitation,

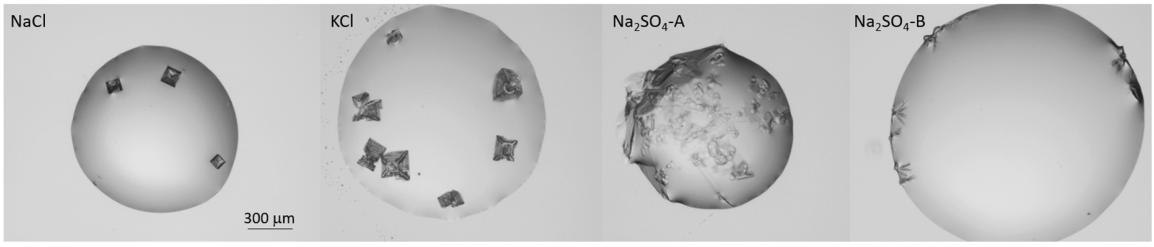

Fig. 8. Location of crystal precipitation at the onset of nucleation and growth in evaporating droplets for the four solutions used in this study.

and the SEM images allow us to observe how these nanocrystals grow under this extreme confinement.

DISCUSSION AND CONCLUSION

We have investigated the initiation and growth of salt creeping by performing salt creep experiments at room temperature, at different relative humidities, on different glass substrates (cylindrical and flat), and for various types of salts and additives. We find that salt creeping on a partially wetting glass substrate occurs during evaporation when the RH is sufficiently low to allow high evaporation rates and multiple nucleation at the contact line. For crystals typically growing at the liquid/solid interface, creeping starts immediately; for crystals growing at the liquid/air interface, creeping starts when the contact angle of the liquid meniscus with the substrate drops below a certain critical value. This critical angle is needed for confining the newly grown crystals suspended to the meniscus by capillary forces. We propose a model in which salt creep emerges when crystals get confined near the substrate, between the solid/liquid and liquid/air interface. The critical contact angle for this to happen is determined by the properties of the crystals nucleating at the liquid/air interface and the surface tension of the solution and is independent of the curvature of the substrate. For pure salts, the lower the surface tension of the salt solution, the smaller this critical angle and the typical size of the confined crystal.

Multiple nucleation at the evaporation front is found to occur at high evaporation rates (i.e., a low RH) and is enhanced by adding crystallization promoters. The multiple nucleation causes crystals to grow beyond the evaporation front, where they provide a platform for a film of solution to extend even further, well beyond the creeping front. Evaporation from this film, in turn, can induce the precipitation of nanocrystals as far as centimeters away from the creeping front. Salt crystallization can, thus, be used as a probe to reveal the extent of precursor nanofilms ahead of a macroscopic front; this result is rather unexpected as we expect that high evaporation rates should rather disrupt any thin films of solution. After its initiation, salt creeping is found to be a self-amplifying process with an exponential growth rate for all salts used in this study, underlining the universality of the process.

We also show that salt creeping can consequently be controlled by influencing the number of emerging crystals (i.e., the branching of the crystallization pattern) and their size. We show that low concentrations of surfactants, around the CMC, can be used to influence the creeping process. In a highly concentrated salt solution, surfactants are found to act as crystallization modifiers rather than wetting agents. We find that additives that promote crystallization cause the creeping process to initiate much earlier in time and accelerate its exponential growth. Additives that inhibit crystallization at the liquid/air interface can be used to avoid salt creeping even at high evaporation rates.

MATERIALS AND METHODS

To determine the impact of the solubility of the salt and the interfacial properties of the emerging crystals on salt creeping, experiments were conducted for three different salts: NaCl, KCl, and Na_2SO_4. These salts were selected first because of their importance in many natural and industrial processes, and second because they have different crystalline structures and different interfacial properties. Sodium chloride (NaCl) and potassium chloride (KCl) generally form cubic anhydrous crystals. Sodium sulfate (Na_2SO_4), on the other hand, has anhydrous (known as thenardite) and hydrated (hepta- and decahydrates) crystalline polymorphs. The decahydrate (known as mirabilite) is the more stable hydrated form of sodium sulfate.

To control the precipitation of either the hydrated (mirabilite) or anhydrous (thernadite) form of sodium sulfate during the experiment, undersaturated salt solutions were prepared on the basis of the equilibrium phase diagram of sodium sulfate at 21° and 35°C (see the Supplementary Materials for details). We referred to these solutions as Na_2SO_4-A and Na_2SO_4-B, respectively. The location of crystallization for each salt was confirmed by performing droplet evaporation experiments in the laboratory at room temperature and an RH of 50%. The results are in good agreement with our previous study (*11*).

As it can be seen in Fig. 8, the NaCl, KCl, and hydrated crystals of sodium sulfate (Na_2SO_4-A) precipitate at the liquid/air interface. The deformation of the liquid/air interface due to the needle-like structure of the hydrated crystals can also be seen in the figure. The anhydrous form of sodium sulfate, thenardite (Na_2SO_4-B), nucleates and grows at the contact line of the droplet with the substrate.

Salt creeping experiments were carried out on a cleaned vertical smooth (cylindrical or flat) glass substrate in contact with a reservoir of an evaporating (initially undersaturated) salt solution (supersaturation $S = m_i/m_s = 0.9$, with m_i and m_s as the initial concentration and the saturation concentration of the salt, respectively). In this way, a continuous supply of the salt solution was achieved, similar as what happens, e.g., in buildings or in soil, when a material is in contact with a salt solution reservoir. The glass substrates were only cleaned with ultrapure water and ethanol to avoid any irreproducible results due to changes in surface chemistry (and therefore the wettability) with aging of treatments such as Piranha cleaning or plasma treatment.

With our experimental setup, we were able to follow the evolution of the contact line of the evaporating salt solution on the glass substrate and the solution's contact angle with the substrate. In addition, by following the mass of the suspended vertical cylinder

with time, if creeping initiated, its rate of growth (i.e., rate of crystal precipitation on the substrate) could be determined (see the Supplementary Materials).

SUPPLEMENTARY MATERIALS

Supplementary material for this article is available at http://advances.sciencemag.org/cgi/content/full/5/12/eaax1853/DC1

Supplementary Materials and Methods

Table S1. Properties of the salt solutions studied.

Fig. S1. Phase diagram of Na_2SO_4 in water as a function of temperature (*9*).

Fig. S2. Influence of surfactants, CTAB and Tween 80, on the nucleation of NaCl.

Fig. S3. Influence of the surfactants on the wetting properties.

Fig. S4. Experimental setup.

Fig. S5. Initiation and growth of salt creeping during the evaporation.

Fig. S6. Evolution of the contact line.

Fig. S7. Evolution of the contact angle up to creeping.

Fig. S8. Effect of the curvature of the glass rod.

Fig. S9. Mass of the salt creep (normalized).

Fig. S10. Experiment of creeping of NaCl and Na_2SO_4 on the glass slide.

Fig. S11. Salts creeping on glass slide.

Movie S1. NaCl solution—Zoom at the contact line.

Movie S2. NaCl + CTAB solution—General view of salt creeping.

Movie S3. Na_2SO_4-B—General view of salt creeping of the anhydrous sodium sulfate (thenardite).

Reference (*25*)

REFERENCES AND NOTES

1. R. Hienonen, R. Lahtinen, *Corrosion and Climatic Effects in Electronics* (VTT Technical Research Centre of Finland, 2000).
2. B.-J. Huang, J.-C. Huang, Creeping-film phenomenon of potassium chloride solution. *Nature* **261**, 36–38 (1976).
3. M. G. Pitman, A. Läuchli, Global impact of salinity and agricultural ecosystems, in *Salinity: Environment - Plants - Molecules* (Kluwer Academic Publishers, Dordrecht, 2002), pp. 3–20.
4. S. M. Green, R. Machin, M. S. Cresser, Long-term road salting effects on dispersion of organic matter from roadside soils into drainage water. *Chem. Ecol.* **24**, 221–231 (2008).
5. R. Hird, M. D. Bolton, Migration of sodium chloride in dry porous materials. *Proc. R. Soc. A Math. Phys. Eng. Sci.* **472**, 20150710 (2016).
6. E. R. Washburn, The creeping of solutions. *J. Phys. Chem.* **31**, 1246–1248 (1926).
7. T. H. Hazlehurst Jr., H. C. Martin, L. Brewer, The creeping of saturated salt solutions. *J. Phys. Chem.* **40**, 439–452 (1935).
8. W. J. P. van Enckevort, J. H. Los, On the creeping of saturated salt solutions. *Cryst. Growth Des.* **13**, 1838–1848 (2013).
9. M. Steiger, S. Asmussen, Crystallization of sodium sulfate phases in porous materials: The phase diagram Na_2SO_4–H_2O and the generation of stress. *Geochim. Cosmochim. Acta* **72**, 4291–4306 (2008).
10. J. W. Mullin, *Crystallization* (Elsevier, 2001).
11. N. Shahidzadeh-Bonn, S. Rafaï, D. Bonn, G. Wegdam, Salt crystallization during evaporation: Impact of interfacial properties. *Langmuir* **24**, 8599–8605 (2008).
12. N. Shahidzadeh, M. F. L. Schut, J. Desarnaud, M. Prat, D. Bonn, Salt stains from evaporating droplets. *Sci. Rep.* **5**, 10335 (2015).
13. D. Bonn, J. Eggers, J. Indekeu, J. Meunier, E. Rolley, Wetting and spreading. *Rev. Mod. Phys.* **81**, 739–805 (2009).
14. A. Naillon, P. Duru, M. Marcoux, M. Prat, Evaporation with sodium chloride crystallization in a capillary tube. *J. Cryst. Growth* **422**, 52–61 (2015).
15. J. Bico, U. Thiele, D. Quéré, Wetting of textured surfaces. *Colloids Surfaces A Physicochem. Eng. Asp.* **206**, 41–46 (2002).
16. P. Meakin, Diffusion-controlled cluster formation in 2—6-dimensional space. *Phys. Rev. A* **27**, 1495–1507 (1983).
17. E. R. Townsend, F. Swennenhuis, W. J. P. van Enckevort, J. A. M. Meijer, E. Vlieg, Creeping: An efficient way to determine the anticaking ability of additives for sodium chloride. *CrstEngComm* **18**, 6176–6183 (2016).
18. M. J. Qazi, R. W. Liefferink, S. J. Schlegel, E. H. G. Backus, D. Bonn, N. Shahidzadeh, Influence of surfactants on sodium chloride crystallization in confinement. *Langmuir* **33**, 4260–4268 (2017).
19. M. J. Qazi, D. Bonn, N. Shahidzadeh, Drying of salt solutions from porous media: Effect of surfactants. *Transp. Porous Media* **128**, 881–894 (2018).
20. P. G. de Gennes, Wetting: Statics and dynamics. *Rev. Mod. Phys.* **57**, 827–863 (1985).
21. M. N. Popescu, G. Oshanin, S. Dietrich, A.-M. Cazabat, Precursor films in wetting phenomena. *J. Phys. Condens. Matter* **24**, 243102 (2012).
22. J. Aizenberg, A. J. Black, G. M. Whitesides, Control of crystal nucleation by patterned self-assembled monolayers. *Nature* **398**, 495–498 (1999).
23. H. Zhang, Z. Wu, L. F. Francis, Formation of salt crystal whiskers on porous nanoparticle coatings. *Langmuir* **26**, 2847–2856 (2010).
24. E. Amstad, M. Gopinadhan, C. Holtze, C. O. Osuji, M. P. Brenner, F. Spaepen, D. A. Weitz, Production of amorphous nanoparticles by supersonic spray-drying with a microfluidic nebulator. *Science* **349**, 956–960 (2015).
25. R. V. Craster, O. K. Matar, On autophobing in surfactant-driven thin films. *Langmuir* **23**, 2588–2601 (2007).

Acknowledgments: We thank D. Bonn for the helpful discussions, and P. Kolpakov and H. Hendrikse (AMOLF) for help in acquiring high-resolution SEM images. **Funding:** The authors acknowledge that they received no funding in support of this research. **Author contributions:** N.S. designed the research. M.J.Q., H.S., C.A.W.D., and E.J.-P. performed the experiments. All authors contributed to the data interpretation and the writing of the paper. **Competing interests:** The authors declare that they have no competing interests. **Data and materials availability:** All data needed to evaluate the conclusions in the paper are present in the paper and/or the Supplementary Materials. Additional data related to this paper may be requested from the authors.

Submitted 1 March 2019
Accepted 30 October 2019
Published 20 December 2019
10.1126/sciadv.aax1853

Citation: M. J. Qazi, H. Salim, C. A. W. Doorman, E. Jambon-Puillet, N. Shahidzadeh, Salt creeping as a self-amplifying crystallization process. *Sci. Adv.* **5**, eaax1853 (2019).